Defect mechanism of $Bi_XSb_{2-X}Te_3$ alloy catalyst for lithium-oxygen battery applications

Songyan Liu,[a] Xujie Song,[a] Jianhua Zhou,*[a] Jie Gao,[a] Haiqing Qin,[b] Xiaoyang Wang,[c] Jun-Liang Chen,[a] Wenping Liu,[a] Xiaoxu Lei [b] and Lei Miao*[c]

Supporting Information

Table S1. Raw material addition amount for preparing $Bi_XSb_{2-X}Te_3$ alloy materials with different proportions

Sample	$BiCl_3$/g	$SbCl_3$/g	Te/g
Bi_2Te_3	1.2615		0.76637
$Bi_{0.7}Sb_{1.3}Te_3$	0.44153	0.59331	0.76637
$Bi_{0.6}Sb_{1.4}Te_3$	0.37846	0.63895	0.76637
$Bi_{0.5}Sb_{1.5}Te_3$	0.31538	0.68459	0.76637
Sb_2Te_3		0.91278	0.76637

Table S2. Grain size of $Bi_xSb_{2-x}Te_3$ alloy material

Sample	Θ	FWHM	D/nm
Bi_2Te_3-(0 1 5)	13.83319	0.19524	43.90842
Bi_2Te_3-(1 0 10)	18.95934	0.39534	22.25786
$Bi_{0.7}Sb_{1.3}Te_3$-(0 1 5)	14.01864	0.36757	23.34078
$Bi_{0.7}Sb_{1.3}Te_3$-(1 0 10)	19.06364	0.39922	22.06014
$Bi_{0.6}Sb_{1.4}Te_3$-(0 1 5)	14.08573	0.49585	17.30742
$Bi_{0.6}Sb_{1.4}Te_3$-(1 0 10)	19.13627	0.44761	19.68391
$Bi_{0.5}Sb_{1.5}Te_3$-(0 1 5)	14.08915	0.34216	25.08187
$Bi_{0.5}Sb_{1.5}Te_3$-(1 0 10)	19.12763	0.36270	24.29075
Sb_2Te_3-(0 1 5)	14.21007	0.16829	51.02268
Sb_2Te_3-(1 0 10)	19.23834	0.21133	41.71760

Table S3. Carrier concentration, the carrier mobility of $Bi_xSb_{2-x}Te_3$ alloy material at 300 K

Sample	Carrier concentration $10^{25}m^{-3}$	Carrier mobility $cm^2V^{-1}s^{-1}$
Bi_2Te_3	1.48	11.3
$Bi_{0.7}Sb_{1.3}Te_3$	1.52	12.8
$Bi_{0.6}Sb_{1.4}Te_3$	1.75	18.1
$Bi_{0.5}Sb_{1.5}Te_3$	1.62	29.1
Sb_2Te_3	1.60	65.8

Table S4. Sample specific surface area, pore volume, and average pore size

Sample	S_{BET} m^2 /g	Pore volume cm^3/g	Average pore size nm
Bi_2Te_3	3.3860	0.035886	42.39241
$Bi_{0.7}Sb_{1.3}Te_3$	4.9389	0.039553	32.03414
$Bi_{0.6}Sb_{1.4}Te_3$	6.5309	0.049508	30.32241
$Bi_{0.5}Sb_{1.5}Te_3$	3.1827	0.017506	22.00170
Sb_2Te_3	2.8324	0.013884	19.60655

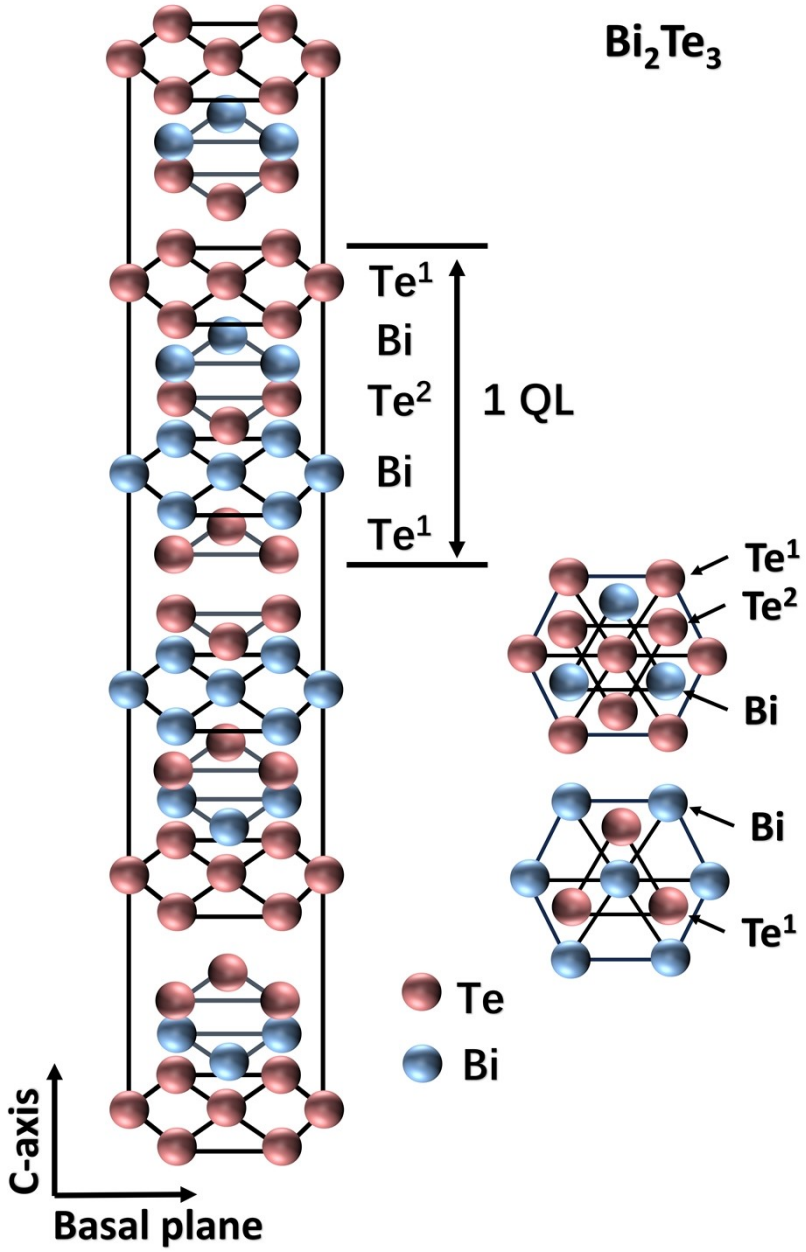

Fig. S1. Schematic cell structure of Bi_2Te_3

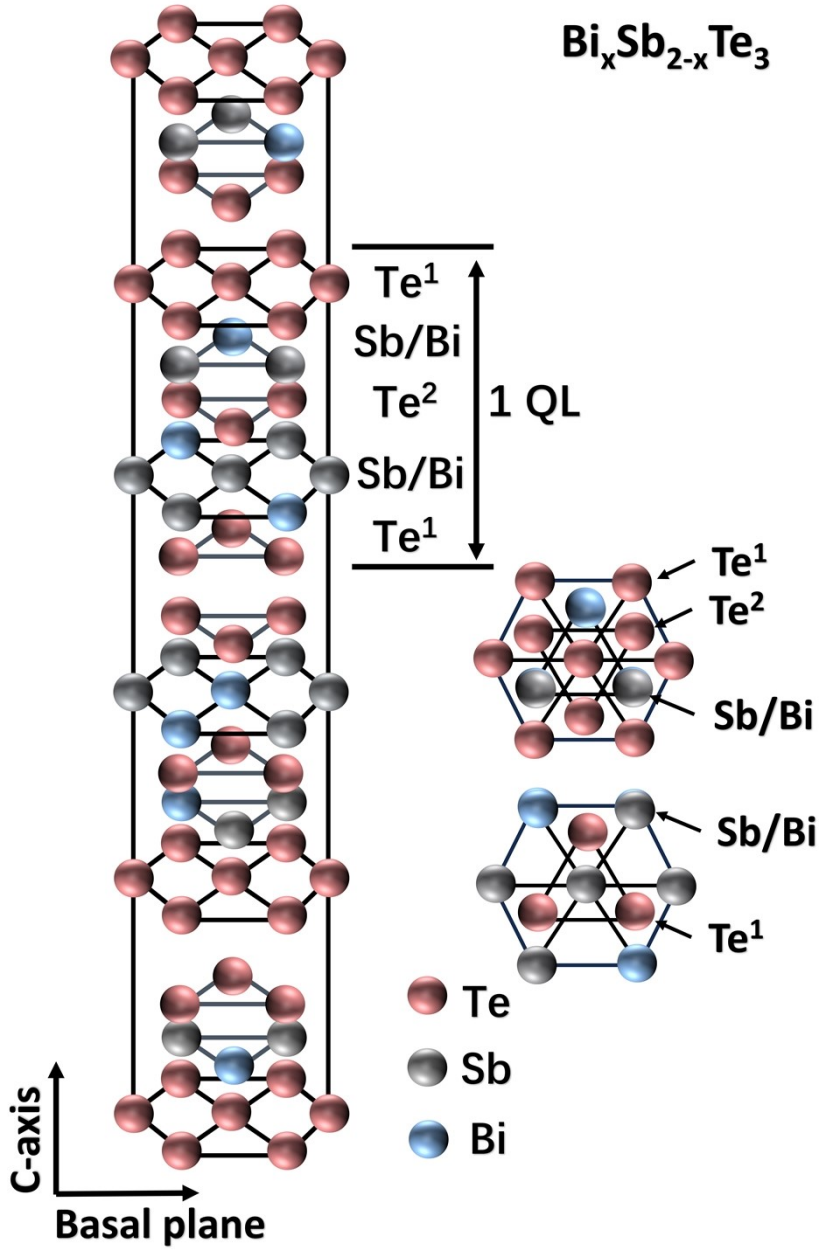

Fig. S2. Schematic cell structure of $Bi_xSb_{2-x}Te_3$

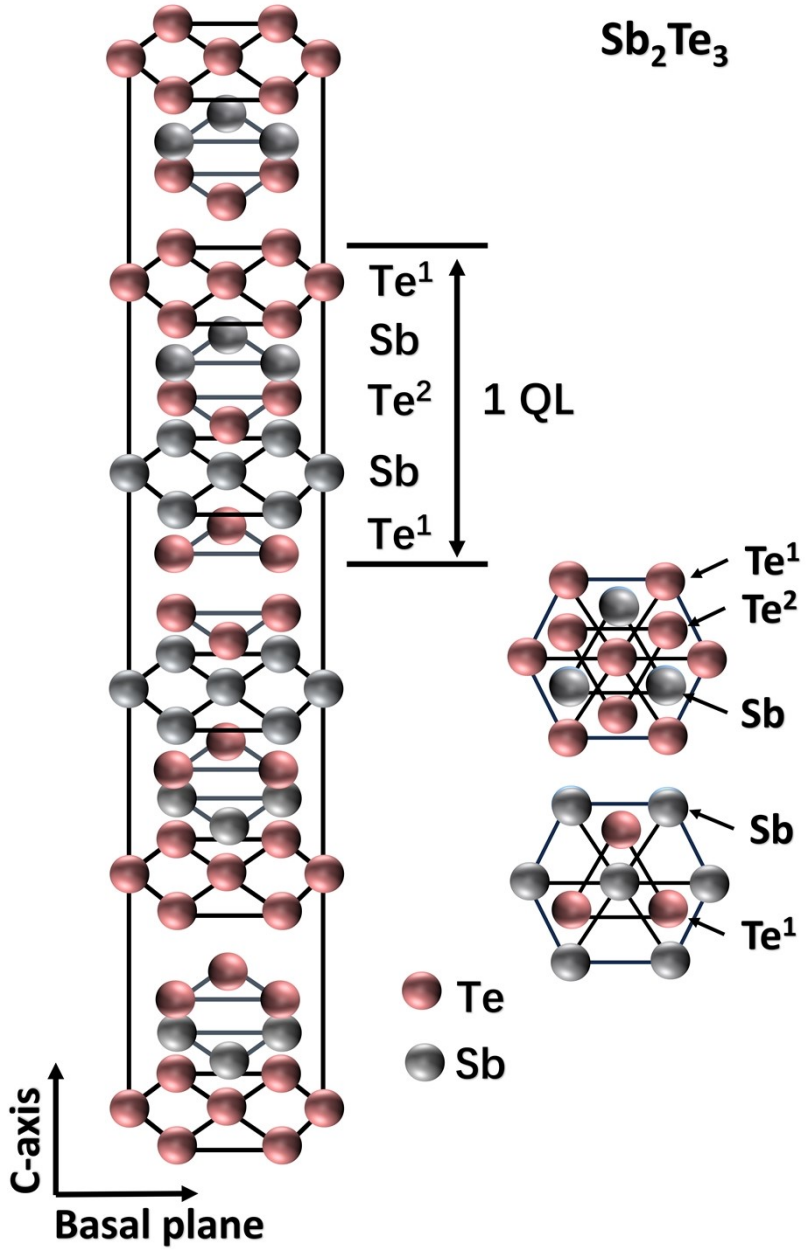

Fig. S3. Schematic cell structure of Sb_2Te_3

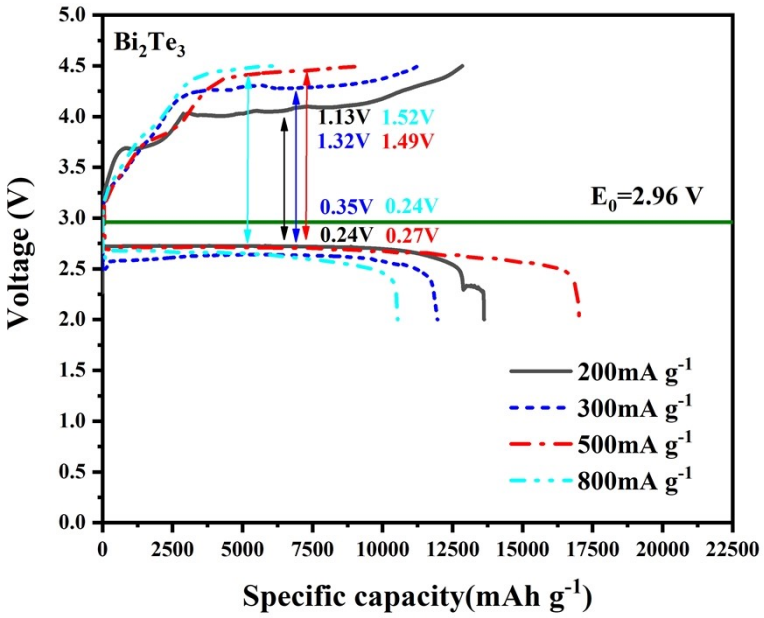

Fig. S4. Initial charge/discharge curves of Bi_2Te_3 alloy material under different current densities

The charge-discharge specific capacities of Bi_2Te_3 cathodes at 200, 300, 500, and 800 $mA{\cdot}g^{-1}$ current densities were demonstrated, in order, 12851.64/13623.08$mAh{\cdot}g^{-1}$, 11283.76/11964.37 $mAh{\cdot}g^{-1}$, 9360.08/17020.05 $mAh{\cdot}g^{-1}$ and 6087.79/10537.57 $mAh{\cdot}g^{-1}$, and the initial Coulombic efficiencies were 94.34%, 94.31%, 54.99% and 57.77%, in that order.

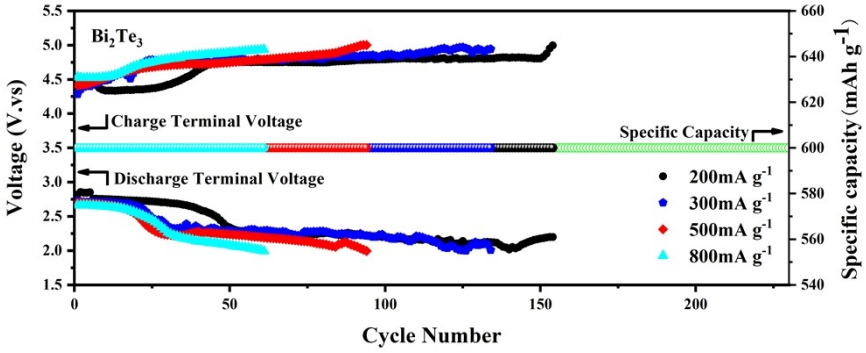

Fig. S5. Charge-discharge termination voltage comparison curves for Bi_2Te_3 cathode at current densities of 200, 300, 500, and 800 mA·g^{-1} and a limited capacity of 600 mAh·g^{-1}

The results showed that the Bi_2Te_3 cathode at 200, 300, 500, and 800 mA·g^{-1} current densities and 600 mAh·g^{-1} fixed cutoff capacity had 154, 134, 94, and 61 cycles in that order.

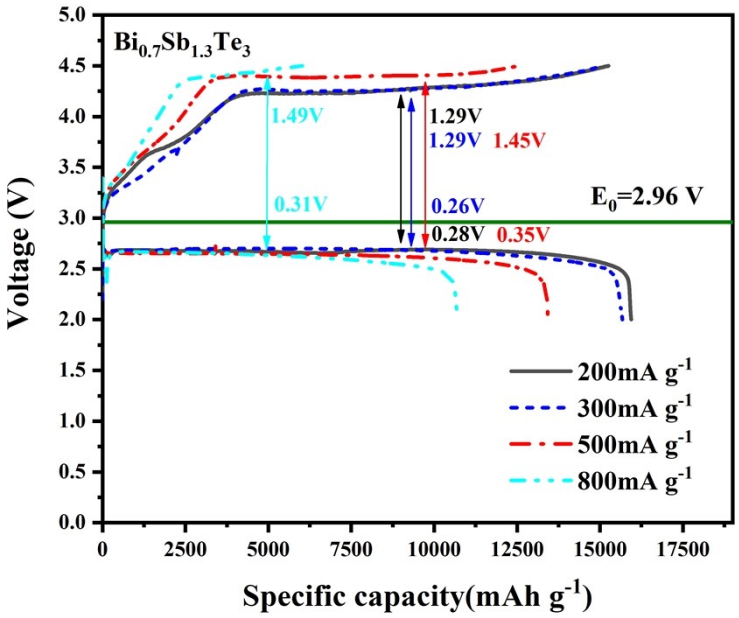

Fig. S6. Initial charge/discharge curves of $Bi_{0.7}Sb_{1.3}Te_3$ alloy material under different current densities

The charge-discharge specific capacities of $Bi_{0.7}Sb_{1.3}Te_3$cathodes at 200, 300, 500, and 800mA·g^{-1} current densities were demonstrated, in order, 15257.76/15941.22 mAh·g^{-1}, 15073.39/15679.30 mAh·g^{-1}, 12527.39/13432.57 mAh·g^{-1} and 6032.02/10701.03 mAh·g^{-1}, and the initial Coulombic efficiencies were 95.71%, 96.14%, 93.26% and 56.37%, in that order.

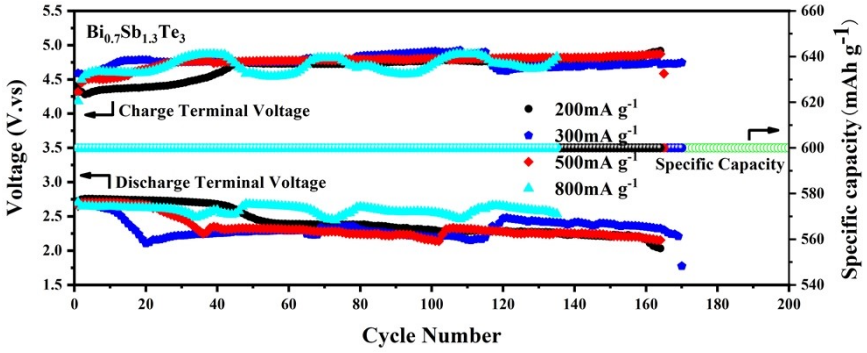

Fig. S7. Charge-discharge termination voltage comparison curves for $Bi_{0.7}Sb_{1.3}Te_3$ cathode at current densities of 200, 300, 500, and 800 $mA{\cdot}g^{-1}$ and a limited capacity of 600 $mAh{\cdot}g^{-1}$

The results showed that the $Bi_{0.7}Sb_{1.3}Te_3$ cathode at 200, 300, 500, and 800 $mA{\cdot}g^{-1}$ current densities and 600 $mAh{\cdot}g^{-1}$ fixed cutoff capacity had 164, 169,164 and 135 cycles in that order.

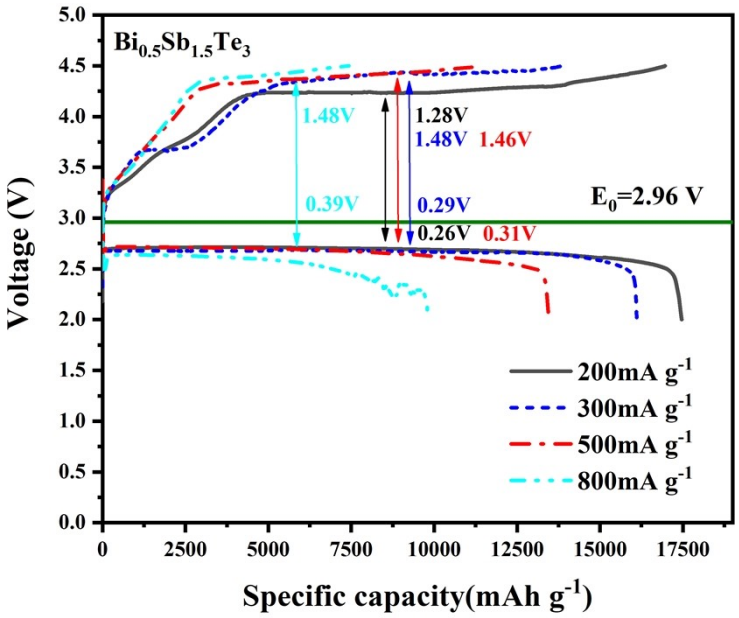

Fig. S8. Initial charge/discharge curves of $Bi_{0.5}Sb_{1.5}Te_3$ alloy material under different current densities

The charge-discharge specific capacities of $Bi_{0.5}Sb_{1.5}Te_3$ cathodes at 200, 300, 500, and 800 $mA{\cdot}g^{-1}$ current densities were demonstrated, in order, 16967.82/17464.59$mAh{\cdot}g^{-1}$, 13900.31/16109.27 $mAh{\cdot}g^{-1}$, 11460.49/13459.38 $mAh{\cdot}g^{-1}$ and 7427.96/9816.18 $mAh{\cdot}g^{-1}$, and the initial Coulombic efficiencies were 97.16%, 86.29%, 85.15% and 75.67%, in that order.

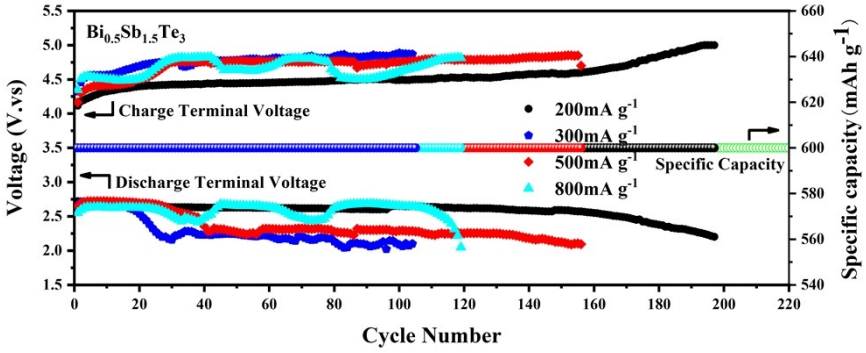

Fig. S9. Charge-discharge termination voltage comparison curves for $Bi_{0.5}Sb_{1.5}Te_3$ cathode at current densities of 200, 300, 500, and 800 $mA \cdot g^{-1}$ and a limited capacity of 600 $mAh \cdot g^{-1}$

The results showed that the $Bi_{0.5}Sb_{1.5}Te_3$ cathode at 200, 300, 500, and 800 $mA \cdot g^{-1}$ current densities and 600 $mAh \cdot g^{-1}$ fixed cutoff capacity had 197, 104, 156 and 119 cycles in that order.

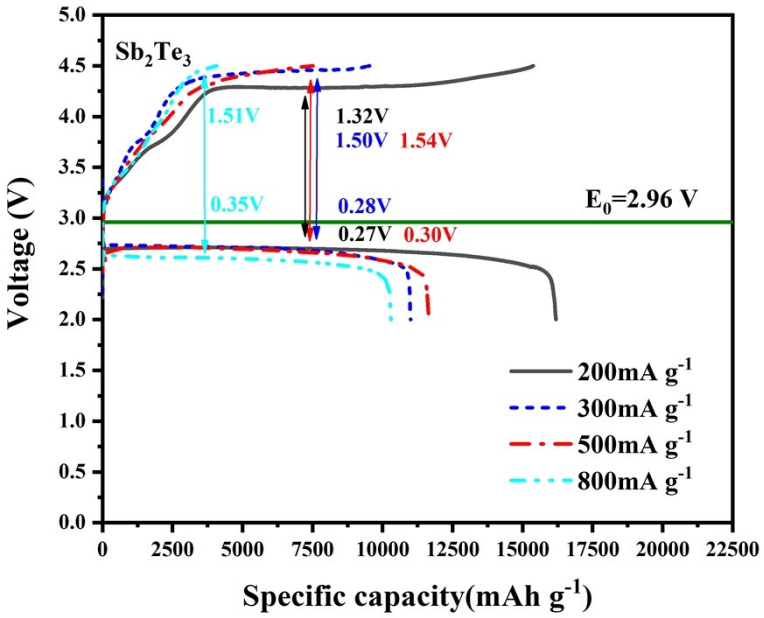

Fig. S10. Initial charge/discharge curves of Sb_2Te_3 alloy material under different current densities

The charge-discharge specific capacities of Sb_2Te_3 cathodes at 200, 300, 500, and 800 mA·g^{-1} current densities were demonstrated, in order, 15381.92/16191.97 mAh·g^{-1}, 9542.12/11005.75 mAh·g^{-1}, 7513.45/11663.70 mAh·g^{-1} and 4077.75/10300.10 mAh·g^{-1}, and the initial Coulombic efficiencies were 95%, 86.70%, 64.42% and 39.59%, in that order.

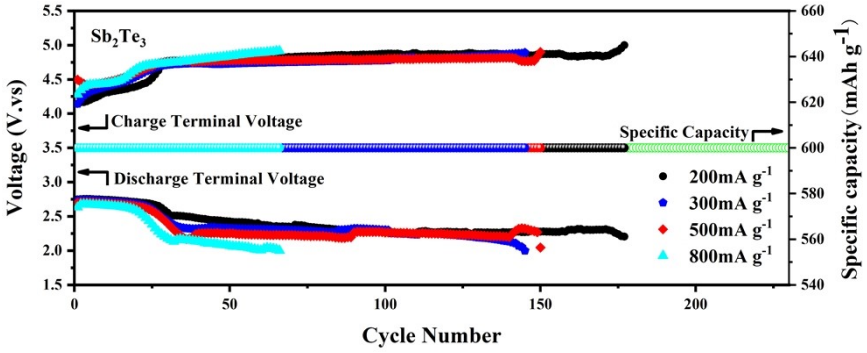

Fig. S11. Charge-discharge termination voltage comparison curves for Sb_2Te_3 cathode at current densi-ties of 200, 300, 500, and 800 mA·g^{-1} and a limited capacity of 600 mAh·g^{-1}

The results showed that the Sb_2Te_3 cathode at 200, 300, 500, and 800 mA·g^{-1} current densities and 600 mAh·g^{-1} fixed cutoff capacity had 177, 145, 150, and 66 cycles in that order.

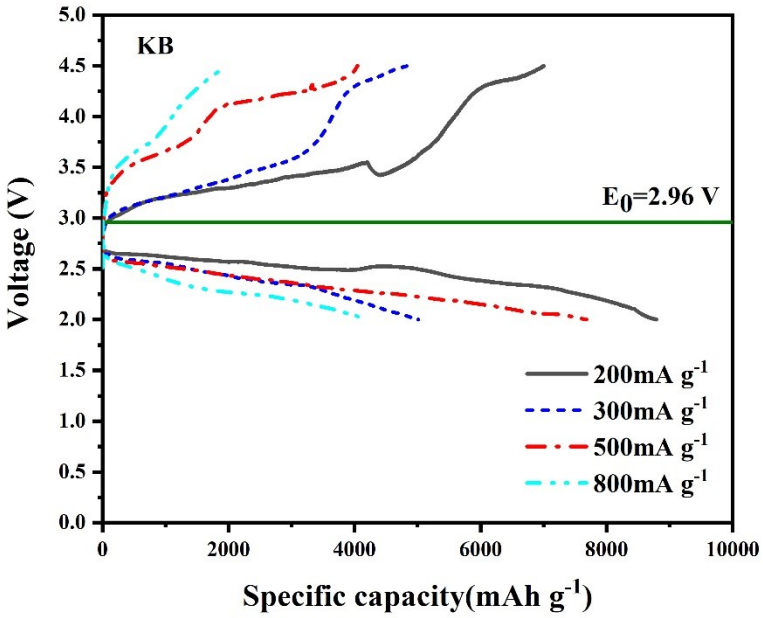

Fig. S12. Initial charge/discharge curves of KB alloy material under different current densities

The charge-discharge specific capacities of KB cathodes at 200, 300, 500, and 800 mA·g^{-1} current densities were demonstrated, in order, 7006.95/8794.92 mAh·g-^{1},4834.88/5015.05 mAh·g^{-1}, 4046.15/7681.45 mAh·g^{-1} and 1962.25/4205.83 mAh·g^{-1}, and the initial Coulombic efficiencies were 79.67%, 96.41%, 52.67% and 46.66%, in that order.

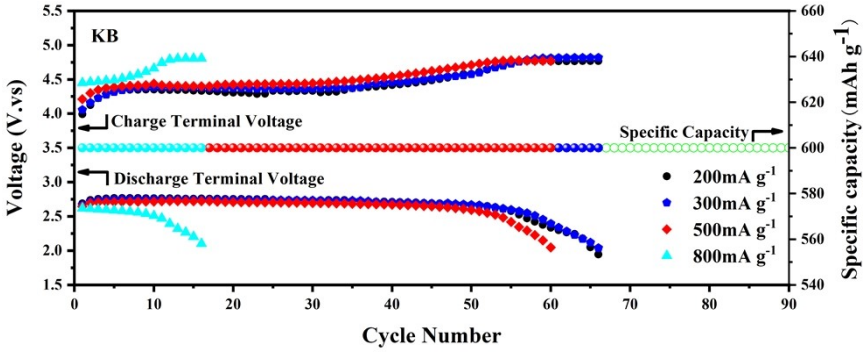

Fig. S13. Charge-discharge termination voltage comparison curves for KB cathode at current densi-ties of 200, 300, 500, and 800 mA·g^{-1} and a limited capacity of 600 mAh·g^{-1}

The results showed that the KB cathode at 200, 300, 500, and 800 mA·g^{-1} current densities and 600 mAh·g^{-1} fixed cutoff capacity had 66, 66, 60, and 16 cycles in that order.

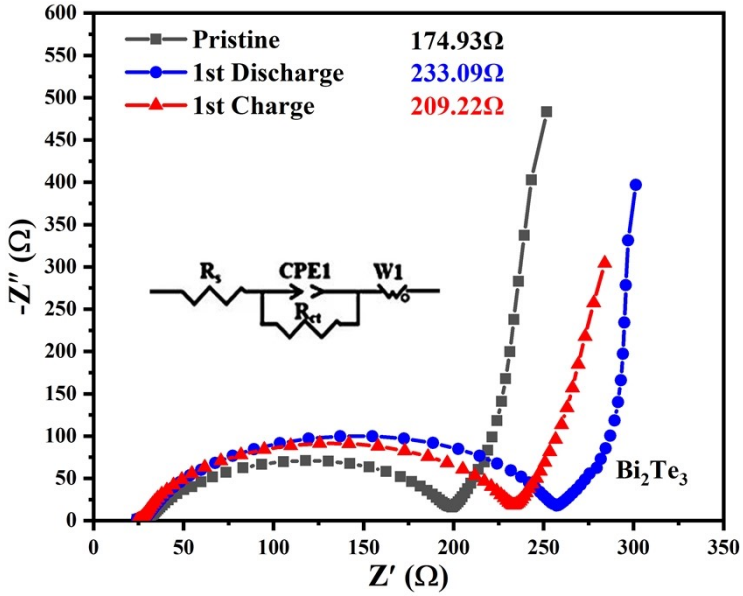

Fig. S14. Nyquist plots of Bi_2Te_3 electrodes at different stages.

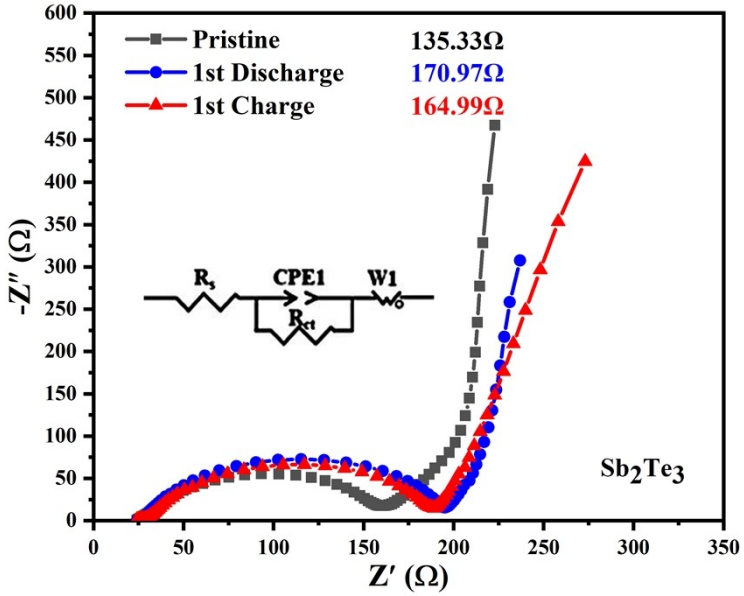

Fig. S15. Nyquist plots of Sb_2Te_3 electrodes at different stages.